CAE-Based Lightweight and Structural Optimization of a Battery Frame for Pure Electric Heavy-Duty Trucks

Bin Chen
School of Mechanical Engineering, Hunan Mechanical & Electrical Polytechnic, Changsha, China
chenbin19870908@163.com

Meng Tang
School of Mechanical Engineering, Hunan Mechanical & Electrical Polytechnic, Changsha, China
tmdawntangmeng@163.com (corresponding author)

Xiangli Lu
School of Mechanical Engineering, Hunan Mechanical & Electrical Polytechnic, Changsha, China
luxiangli1983@gmail.com

Received: 5 March 2026 | Revised: 6 April 2026 | Accepted: 17 April 2026

 DOI: https://doi.org/10.48084/etasr.18536

ABSTRACT

Pure-electric heavy-duty trucks require lightweight, reliable battery frames to improve payload capacity and operational efficiency. In this study, a battery frame for a pure electric heavy-duty truck was optimized using a Computer-Aided Engineering (CAE)-based design methodology. Static strength and modal analyses were first performed to identify structural redundancy and stiffness deficiencies. Based on these results, a comprehensive optimization strategy integrating topology optimization, size optimization, aluminum alloy material substitution, and CAE verification was applied to the upper frame, base tray, subframe, and connecting components. The optimized battery frame achieves 164 kg mass reduction, corresponding to 24% lightweight rate, while meeting strength and stiffness requirements across all critical working conditions. The maximum deformation is reduced by 41%, and the first-order natural frequency increases by 28.8%, effectively avoiding resonance within typical road excitation frequency ranges. The results demonstrate significant improvements in both static and dynamic performance, indicating the effectiveness of the proposed optimization strategy. Physical safety performance tests are planned to further validate the feasibility and engineering applicability of the optimized design.

Keywords-CAE simulation; lightweight optimization; topology optimization; pure electric heavy-duty truck

I. INTRODUCTION

The power battery frame serves as a core load-bearing and protective structure in pure electric trucks, and its structural reliability is significant for ensuring battery durability and vehicle safety. Due to its relatively large mass, the battery frame generally accounts for approximately 6%–8% of the total vehicle mass, which has a direct impact on payload capacity and operational economic performance [1-3]. Furthermore, while the original symmetric structural response characteristics are retained, the overall mass of the frame is significantly reduced from 81 kg to 68 kg [4]. As the primary load-bearing and protective structure of the battery pack, the battery frame is required to withstand complex service loads, including vibration, impact, and torsion during vehicle operation, as well as long-term fatigue induced by continuous vibration. Consequently, the rationality of the battery frame design is substantial to the overall functionality, durability, and reliability of the vehicle.

To meet the requirements of long-distance transportation and heavy-load logistics, the capacity and mass of power batteries for pure electric trucks have continuously increased, resulting in larger battery frames and higher demands on their strength and reliability [5].

Studies on the lightweight design of battery frames have been conducted. Authors in [6] investigated a battery enclosure manufactured from 5052 aluminum alloy, achieving effective weight reduction while maintaining adequate structural strength. Authors in [7] optimized a battery frame using the response surface methodology by replacing steel with aluminum and reinforcing the structure with glass fiber sheet molding compounds, resulting in a 29.7% weight reduction under comparable stress levels. Authors in [8] adopted a top–

down design methodology combined with topology optimization to develop a lightweight composite battery pack enclosure featuring cross-shaped stiffening ribs. Despite these advances, existing studies are predominantly focused on battery frames for passenger electric vehicles. Research addressing the lightweight optimization of battery frames for pure electric trucks, particularly under high-load conditions, and a complex operating environment remains relatively limited. Moreover, systematic experimental validation of the structural safety and reliability of optimized battery frames is often insufficient, which restricts their practical engineering application.

In this study, the battery frame of a pure electric heavy-duty truck is selected as the research object. Computer-Aided Engineering (CAE) simulations are first conducted to evaluate structural strength and vibration characteristics, enabling the identification of design redundancies. Subsequently, a comprehensive optimization strategy—comprising topology optimization, size optimization, aluminum alloy substitution, and CAE verification—is applied to the upper frame, base tray, subframe, and connecting plates. Finally, bench tests on physical prototypes are planned to validate the feasibility and effectiveness of the optimized design in terms of both reliability and lightweight performance.

II. STATIC AND DYNAMIC PERFORMANCE ANALYSIS OF THE BATTERY FRAME

A. Structural Description of the Original Battery Frame

A pure electric heavy-duty truck with a rear-mounted battery system installed on the chassis frame behind the cab is shown in Figure 1. The battery frame of this type typically weighs 500–800 kg and operates under severe working conditions, significantly affecting both vehicle economy and reliability.

Fig. 1. A pure electric heavy-duty truck with a rear-mounted battery system, showing: (a) chassis frame, (b) power battery assembly, and (c) cab.

The battery system of a pure electric heavy-duty truck comprises battery modules, a battery frame, and protective panels. The battery frame, as the core load-bearing structure, is the focus of this study, as depicted in Figure 2. It consists of an upper frame, base tray, subframe, and connecting plates. The original material is Q345 steel, with overall dimensions of 2400 mm × 900 mm × 1800 mm and a mass of 682 kg. The initial design emphasizes structural stiffness over lightweight performance, necessitating structural optimization to enhance overall performance and reduce weight.

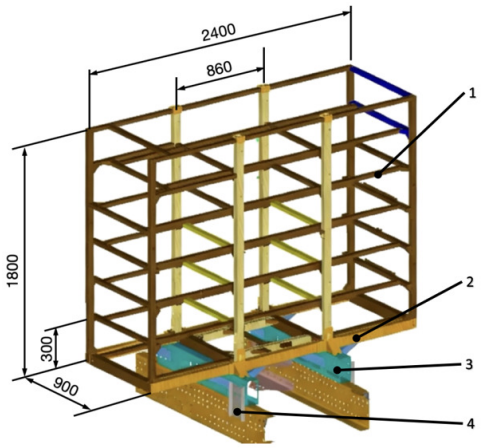

Fig. 2. 3D structure of battery frame, showing: (1) upper frame body, (2) base bracket, (3) subframe, and (4) connecting plate.

B. Finite Element Model Establishment

According to commercial vehicle finite element modeling standards, the model was simplified during preprocessing. Bolts, nuts, and other standard components were removed, and bonded constraints were applied to simulate connections. Non-critical chamfers and fillets were eliminated to reduce mesh density. Welded joints were modeled using equivalent weld models to ensure the accurate simulation of connection strength [9, 10].

A hybrid meshing strategy combining structured and unstructured meshes was adopted. Mid-surfaces were extracted for all structural components. Main load-bearing members, such as longitudinal and cross beams, were meshed with quadrilateral shell elements of 10 mm size, while three-dimensional components, including mounting brackets and stiffeners, were meshed with tetrahedral elements sized 6–10 mm. A mesh refinement to 5 mm was applied in stress concentration regions, such as mounting holes and beam connections. The final finite element model comprised 730,000 nodes and 480,000 elements, with mesh distortion ≤ 0.7 and aspect ratio ≤ 3, satisfying the accuracy requirements [11].

C. Static Analysis

- Working Conditions and Load Settings

During operation, the battery frame is primarily subjected to the weight of the battery, inertial impacts caused by vehicle motion, and torsional loads induced by uneven road surfaces. Based on realistic operating scenarios, such as mountainous roads, emergency braking, and high-speed cornering, four extreme working conditions were selected: diagonal lifting, heavy load, extreme cornering, and emergency braking. Gravitational acceleration was set to $g = 9.8$ m/s^2. The parameters for these working conditions are summarized in Table I.

According to [12, 13], the inertial forces of the battery pack and the torsional loads induced by road conditions were

equivalently applied to the nodes in contact between the battery frame and the battery modules. The total weight of the battery pack was 35,000 N.

TABLE I. EXTREME WORKING CONDITION PARAMETERS OF BATTERY FRAME

Working condition	X-direction acceleration	Y-direction acceleration	Z-direction acceleration
Lifting condition	-	-	Torsion angle: 3°
Heavy load condition	-	-	2g
Extreme turning	-	0.6g	1g
Emergency braking	0.8g	-	1g

- Static Analysis Results

CAE-based finite element simulations were conducted to evaluate the maximum stress and diagonal deformation of the frame openings. The corresponding stress contour plots are presented in Figure 3. The numerical results at different locations under various working conditions are summarized in Table II. The mounting brackets are manufactured from QT400-18 with a yield strength of 400 MPa, whereas the remaining structural components are made of Q345 steel with a yield strength of 345 MPa.

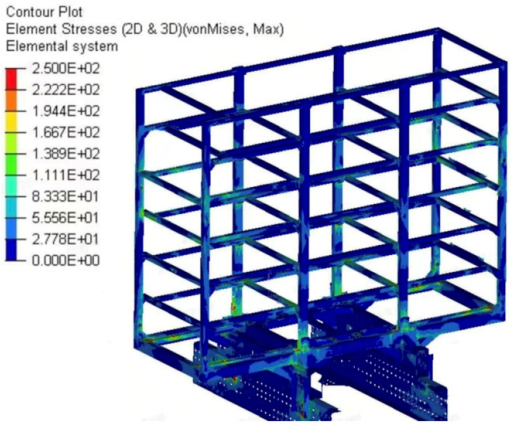

Fig. 3. Stress cloud diagram of static simulation.

The analysis shows that, under all operating conditions, the maximum von Mises stress remains well below the corresponding material yield strengths, indicating that the structure possesses sufficient strength. However, the maximum deformation of the upper frame opening reaches 12 mm, which reveals inadequate structural stiffness. Such excessive deformation may induce additional loads on attached components, potentially leading to failure modes such as battery module cracking and electrolyte leakage. Overall, the results indicate that the original design is overly conservative in terms of material strength selection while failing to provide sufficient stiffness. This imbalance suggests considerable potential for lightweight optimization and stiffness enhancement through structural redesign.

TABLE II. STATIC ANALYSIS OF THE ORIGINAL BATTERY FRAME

Working condition	Upper frame body		Base bracket	Connecting plate
	Max concentrated stress/MPa	Max displacement /mm	Max concentrated stress/MPa	Max concentrated stress/MPa
Lifting condition	218	7.9	250	229
Heavy load condition	169	6.2	148	159
Extreme turning	150	13.2	129	140
Emergency braking	184	16.3	170	185

D. Modal Analysis

The battery frame is connected to the load-bearing chassis frame through bolted joints. To more accurately represent the actual dynamic behavior, a constrained modal analysis was performed by applying full-degree-of-freedom constraints at the mounting holes. The first six natural frequencies and corresponding mode shapes were extracted, and the results are outlined in Table III.

TABLE III. FIRST 6-ORDER MODAL PARAMETERS OF THE ORIGINAL BATTERY FRAME

Order	Mode shape description	Natural frequency/Hz
1	X-direction swing of upper frame top	11.8
2	Y-direction swing of upper frame top	12.5
3	2nd-order X-direction swing of upper frame top	28.2
4	2nd-order Y-direction swing of upper frame top	27.7
5	Z-axis torsion	40.9
6	3rd-order X-direction swing of upper frame top	11.8

During vehicle operation, road-induced excitation frequencies are generally below 12 Hz [14]. The first natural frequency of the original frame is 11.8 Hz, which falls within this excitation range and therefore poses a potential resonance risk. Such resonance may result in fatigue damage to the upper frame, loosening of the battery mounting bolts, and localized structural failures. Consequently, optimization of the upper frame structure is required to increase the natural frequencies and enhance the overall dynamic performance.

III. MULTIDIMENSIONAL OPTIMIZATION DESIGN OF THE BATTERY FRAME

A. Lightweight Material Substitution

For non-load-bearing components, such as protective panels and structural parts with stress levels below 100 MPa, lightweight substitution using aluminum alloys was considered. The 6xxx-series aluminum alloys were selected due to their favorable formability and mechanical performance. The material properties of 6005A and 6063 aluminum alloy are listed in Table IV, with a density only 34.4% that of steel, providing significant potential for weight reduction.

The roof and side panels primarily function as protection against water intrusion and external impacts. Considering functional requirements and manufacturing feasibility, 6063-T5 aluminum alloy profiles were selected for these panels and connected to the upper frame using embedded bolts. In addition, 6005A-T6 aluminum alloy tubular beams were adopted to replace the original diagonal braces. As a result, the mass of the roof and associated tubular components was reduced from 82 kg to 48 kg, achieving a weight reduction of 34 kg.

TABLE IV. MATERIAL PROPERTIES OF 6005A AND 6063 ALUMINUM ALLOY

Material properties	6005A-T6	6063-T5
Elastic modulus (MPa)	6.9×10^4	6.9×10^4
Poisson's ratio	0.3	0.3
Density (kg/m^3)	2700	2700
Yield strength (MPa)	250	110
Tensile strength (MPa)	270	160

B. Topology Optimization

- Optimization Objectives

Topology optimization was performed to reduce structural mass while maintaining sufficient strength. The four side surfaces of the upper frame and the base tray were defined as the design space. The objective function was to minimize mass under the constraints of maximum stress ≤ 224 MPa and maximum deformation ≤ 12 mm, corresponding to a safety factor of 1.5. A density-based topology optimization method was employed.

- Topology Optimization

Based on the topology optimization density contour, significant material redundancy is observed across all four side surfaces of the upper frame. The conventional frame structure exhibits insufficient load-bearing capacity and deformation resistance. Figure 4 shows the material distribution of the optimized left and right sides, where an "X"-shaped load path, analogous to a triangular truss, enhances stiffness in the X-direction and reduces deformation during emergency braking. Similarly, Figure 5 presents the front and rear side material contours with a "W"-shaped load path, which improves Y-direction stiffness and mitigates deformation under extreme turning conditions.

The optimization results reveal the main load transfer paths and indicate substantial material redundancy in the original design. The optimized side surfaces exhibit X-shaped load paths, equivalent to triangular truss structures, which enhance longitudinal stiffness and reduce deformation under emergency braking conditions. The front and rear surfaces display W-shaped load paths, significantly improving lateral stiffness under extreme cornering conditions.

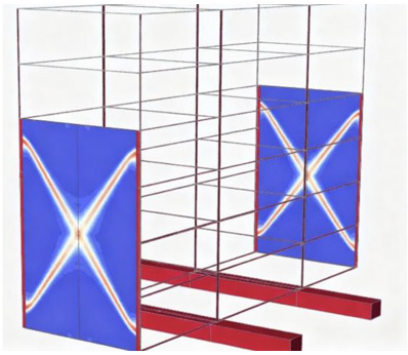

Fig. 4. Topology optimization cloud diagram of the left and right sides of the upper frame body.

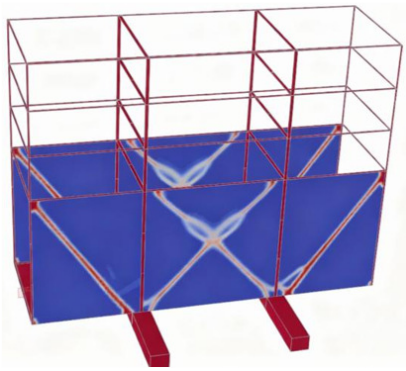

Fig. 5. Topology optimization cloud diagram of the front and rear sides of the upper frame body.

The material distribution of the optimized base bracket is depicted in Figure 6. The upper frame is designed to endure the forces generated during extreme turning and emergency braking. In contrast, the underbody support is tailored specifically for lifting and heavy - load situations. The central part features an "X"-shaped structure, with triangular structures on either side. Together, they create a geometry resembling an inverted carrying pole. This structural design significantly boosts the overall stiffness under heavy loads and efficiently reduces the overall deformation of the frame.

- Size Optimization

Size optimization was applied to components with notable strength redundancy, including the subframe, connecting brackets, and various beams of the upper frame. Component thicknesses were defined as design variables, with the objective of minimizing the total frame mass under the same static performance constraints. The optimized thickness values and corresponding standard material specifications are listed in Table V.

- Model Reconstruction

Based on the results of material substitution, topology optimization, and size optimization, the battery frame was reconstructed. Aluminum alloy diagonal braces were added to the four side surfaces of the upper frame in accordance with the topology-optimized load paths. The base tray was redesigned with transverse beams and profiled cross-sections,

incorporating irregular holes aligned with force transmission paths. The reconstructed three-dimensional model is displayed in Figure 7.

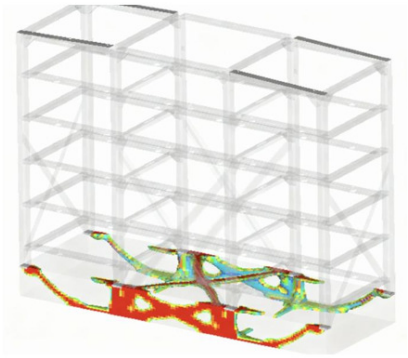

Fig. 6. Topology optimization cloud diagram of the base bracket.

TABLE V. OPTIMIZATION RESULTS OF FRAME COMPONENT SIZES (mm)

Component name	Original thickness	Optimized thickness	Material specification selection
Subframe	12	8.1	8
Connecting bracket	14	9.7	10
X-direction beam of upper frame body	6	5.5	6
Y-direction beam of upper frame body	8	6.8	7
Z-direction longitudinal beam of upper frame body	5	4.8	5

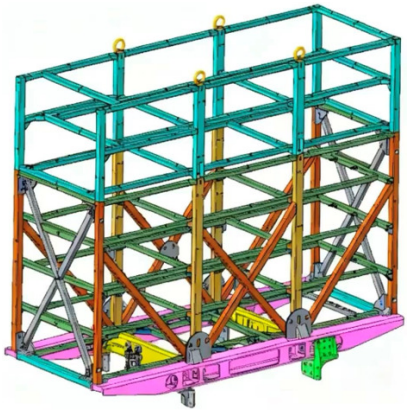

Fig. 7. 3D model reconstruction of the battery frame.

- Performance Comparison Before and After Optimization

Static and modal analyses were conducted on the optimized battery frame. The results demonstrate a significant improvement in structural stiffness and a more uniform stress distribution. The total mass of the battery frame was reduced from 682 kg to 518 kg, corresponding to a weight reduction of 164 kg and a lightweight rate of 24%.

Under identical working conditions and constraints, comparative results of the static and modal analyses before and after optimization are presented in Tables VI and VII.

TABLE VI. STATIC ANALYSIS OF THE OPTIMIZED BATTERY FRAME

Working condition	Upper frame body		Base bracket	Connecting plate
	Max concentrated stress/MPa	Max displacement/ mm	Max concentrated stress/MPa	Max concentrated stress/MPa
Lifting condition	223	6.5	212	197
Heavy load condition	187	5.4	142	158
Extreme turning	189	8.2	148	165
Emergency braking	196	9.6	189	203

TABLE VII. FIRST 6-ORDER MODAL PARAMETERS OF THE OPTIMIZED BATTERY FRAME

Order	Mode shape description	Natural frequency/Hz
1	X-direction swing of upper frame top	15.2
2	Y-direction swing of upper frame top	16.8
3	2nd-order X-direction swing of upper frame top	33.2
4	2nd-order Y-direction swing of upper frame top	32.3
5	Z-axis torsion	43.4
6	3rd-order X-direction swing of upper frame top	46.3

The maximum deformation of the upper frame opening under emergency braking conditions decreased from 16.3 mm to 9.6 mm, representing a 41% reduction. The maximum stress decreased from 250 MPa to 223 MPa, achieving the target safety factor of 1.5.

The first and second natural frequencies increased to 15.2 Hz and 16.8 Hz, respectively, representing improvements of 28.8% and 34.4%. All modal frequencies exceeded 12 Hz, effectively avoiding resonance and significantly improving dynamic performance.

IV. CONCLUSION

This study investigated the structural optimization of a battery frame for a pure-electric heavy-duty truck based on Computer-Aided Engineering (CAE) simulations. The main conclusions are:

- Static and modal analyses indicated that the original battery frame had insufficient stiffness and low natural frequencies, along with significant structural redundancy and a prominent resonance risk within the road excitation frequency range. This not only restricted the frame's performance but also highlighted the need for improvement.
- By implementing a comprehensive optimization strategy integrating material substitution, topology optimization, and

size optimization, the mass of the battery frame was successfully decreased by 164 kg (24%). The first and second natural frequencies were increased to 15.2 Hz and 16.8 Hz, respectively. Compared to the original state, this represented a remarkable enhancement in dynamic performance, effectively eliminating resonance-related failure risks.

- This study not only verifies that topology-driven structural reconstruction and material substitution can effectively address the long-standing conflict between lightweight design and structural reliability for heavy-duty electric truck battery frames but also offers a fresh perspective. The optimized load paths (X-shaped and W-shaped) provide a general and valuable reference for similar load-bearing structures.

Future work will focus on standardizing material thickness selections, as some optimized thickness values (e.g., 7 mm) are not commonly available and may need to be adjusted to standard sizes (e.g., 8 mm), potentially reducing lightweight efficiency. In addition, variations in plate thickness and structural configuration may influence welding manufacturability and require further process validation. Physical prototype testing will also be necessary to verify the practical effectiveness of the optimized design.

DECLARATION OF COMPETING INTERESTS

Not applicable to this work.

ACKNOWLEDGMENT

Not applicable to this work.

DATA AVAILABILITY

Calculated and simulation data are described within the paper.

REFERENCES

[1] F. Jönsson and J. Kindahl, "Packaging concepts of an energy storage system for a fully electric heavy duty truck," M.S. thesis, Dept. of Industrial and Materials Science, Chalmers University of Technology, Gothenburg, Sweden, 2018.

[2] X. Chen, J. Wang, K. Zhao, and L. Yang, "Electric vehicles body frame structure design method: An approach to design electric vehicle body structure based on battery arrangement," in *Proceedings of the Institution of Mechanical Engineers, Part D: Journal of Automobile Engineering*, vol. 236, no. 9, pp. 2025–2042, 2022, https://doi.org/10.1177/09544070211052957.

[3] Z. Song, "Optimized Design Solutions for Battery and Frame Performance and Safety in New Energy Vehicles," *MATEC Web of Conferences*, vol. 404, 2024, Art. no. 01006, https://doi.org/10.1051/matecconf/202440401006.

[4] Y. Liu, C. Liu, X. Gao, and J. Tan, "Multiphysics Finite Element Analysis and Optimization of Load-Bearing Frame for Pure Electric SUVs," *Symmetry*, vol. 17, no. 7, 2025, Art. no. 1143, https://doi.org/10.3390/sym17071143.

[5] C. J. Chng, "A Feasibility Study on Utilising High-Performance Lithium-ion Capacitor as Main Power Source for Electric Lorries," M.S. thesis, Department of Mechanical and Aerospace Engineering, University of Strathclyde, Glasgow, Scotland, 2019.

[6] S. Kaleg and Amin, "1P15S lithium battery pack: Aluminum 5052-0 strength of material analysis and optimization," in *2016 International Conference on Sustainable Energy Engineering and Application (ICSEEA)*, Jakarta, Indonesia, Oct. 03–05, 2016, pp. 1–5, https://doi.org/10.1109/ICSEEA.2016.7873558.

[7] S. J. Hwang, M. S. Oh, O. C. Sul, M. G. Yoo, Y. G. Chung, and S. moo Hong, "Design of a Lightweight Model for the Battery Carrier of a Commercial Large Electric Truck Using the Response Surface Method," *Journal of the Korean Society of Manufacturing Technology Engineers (KSMTE)*, vol. 32, no. 5, pp. 283–288, Oct. 2023, https://doi.org/10.7735/ksmte.2023.32.5.283.

[8] X. Zhang *et al*., "Top-Down Design Approach of Lightweight Composite Battery Pack Enclosure for Electric Vehicles Based on Numerical Modeling and Topology Optimization," *Polymers*, vol. 17, no. 21, 2025, Art. no. 2897, https://doi.org/10.3390/polym17212897.

[9] J. Peng, C. Hou, and L. Shen, "Numerical simulation of weld fracture using cohesive interface for novel inter-module connections," *Journal of Constructional Steel Research*, vol. 174, Nov. 2020, Art. no. 106302, https://doi.org/10.1016/j.jcsr.2020.106302.

[10] M. S. Liu, C. A. Li, J. R. Huang, and J. S. Ju, "Numerical Modeling and Mechanical Analysis of Combined Connection with Bolts and Welds," *Strength of Materials*, vol. 48, no. 6, pp. 862–869, Nov. 2016, https://doi.org/10.1007/s11223-017-9832-1.

[11] J. Zhang, B. He, R. Nie, G. Wang, L. Zhang, and X. Ma, "Optimal self-stress determination for high-accuracy mesh reflectors design considering the pillow distortion," *Structures*, vol. 59, Jan. 2024, Art. no. 105736, https://doi.org/10.1016/j.istruc.2023.105736.

[12] R. Zhang, Y. Duan, F. Zhang, and Y. Liao, "Ground Impact Analysis of the Battery Pack Based on the Whole Vehicle Model," *SAE International*, Apr. 2023, https://doi.org/10.4271/2023-01-0778.

[13] D. Qin, P. Wang, T. Wang, and J. Chen, "Modeling and Dynamic Impact Analysis of Prismatic Lithium-Ion Battery," *Sustainability*, vol. 15, no. 10, 2023, Art. no. 8414, https://doi.org/10.3390/su15108414.

[14] M. Kúdelčíková and J. Melcer, "Properties of road unevenness inducing the kinematical excitation of vehicles," *MATEC Web of Conferences*, vol. 107, 2017, Art. no. 00028, https://doi.org/10.1051/matecconf/201710700028.